Enhancing the "A-Rule" of Translesion DNA Synthesis: Promutagenic DNA Synthesis Using Modified Nucleoside Triphosphates†

Babho Devadoss,‡ Irene Lee,‡ and Anthony J. Berdis*,§

Departments of Chemistry and Pharmacology, Case Western Reserve University, 10900 Euclid Avenue, Cleveland, Ohio 44106

Received July 5, 2007; Revised Manuscript Received September 6, 2007

ABSTRACT: Abasic sites are mutagenic DNA lesions formed as a consequence of inappropriate modifications to the functional groups present on purines and pyrimidines. In this paper we quantify the ability of the high-fidelity bacteriophage T4 DNA polymerase to incorporate various promutagenic alkylated nucleotides opposite and beyond this class of non-instructional DNA lesions. Kinetic analyses reveal that modified nucleotides such as N^6-methyl-dATP and O^6-methyl-dGTP are incorporated opposite an abasic site far more effectively than their unmodified counterparts. The enhanced incorporation is caused by a 10-fold increase in k_{pol} values that correlates with an increase in hydrophobicity as well as changes in the tautomeric form of the nucleobase to resemble adenine. These biophysical features lead to enhanced base-stacking properties that also contribute toward their ability to be easily extended when paired opposite the non-instructional DNA lesion. Surprisingly, misincorporation opposite templating DNA is not enhanced by the increased base-stacking properties of most modified purines. The dichotomy in promutagenic DNA synthesis catalyzed by a high-fidelity polymerase indicates that the dynamics for misreplicating a miscoding versus a non-instructional DNA lesion are different. The collective data set is used to propose models accounting for synergistic enhancements in mutagenesis and the potential to develop treatment-related malignancies as a consequence of utilizing DNA-damaging agents as chemotherapeutic agents.

DNA polymerases play an essential role in maintaining genomic integrity by faithfully copying the template strand of nucleic acid. Most models of polymerization fidelity attribute the veracious transmission of genetic information to the formation of Watson−Crick hydrogen-bonding interactions between the incoming nucleotide and the templating base (reviewed in ref *1*). Unfortunately, the functional groups that provide these energetically favorable interactions are highly susceptible to modifications by various DNA-damaging agents (reviewed in ref *2*). For example, alkylating agents such as methyl methanesulfonate, dimethylnitrosamine, and *N*-methyl-*N*′-nitro-*N*-nitrosoguanidine have been shown to preferentially react with the N3- and N7-positions of adenine in addition to the O6-position of guanine (*3*−*5*). These inappropriate modifications can alter the hydrogen-bonding potential of a templating base to cause mutagenesis (*6*, *7*) and induce carcinogenesis (*8*−*10*).

In addition to the aforementioned modifications, alkylating agents can also create abasic sites that can arise from the hydrolysis of a N−glycosidic bond that occurs either nonenzymatically (*11*, *12*) or via the action of various DNA glycosylases (*13*−*15*). The noninstructional nature of an abasic site predicts that it would act primarily as a strong block for DNA synthesis. However, numerous in vitro and in vivo studies demonstrated that dATP is preferentially incorporated opposite an abasic site by various DNA polymerases (*16*−*20*). This kinetic phenomenon is commonly referred to as the "A-rule" of translesion DNA synthesis (reviewed in ref *21*). Our mechanistic studies using the high-fidelity DNA polymerase from bacteriophage T4 (gp43) demonstrated that dATP is incorporated opposite an abasic site ∼100-fold more efficiently than other natural nucleotides (*22*). This enhancement is caused through a combination of higher binding affinity coupled with an increase in the rate constant for polymerization of dATP compared to the other natural nucleotides (*22*).

Most reports evaluating the effects of various DNA-damaging agents have focused on studying promutagenic DNA synthesis caused by misreplication of the modified templating strand. However, the impact of these alkylating agents is not solely confined to DNA as nucleoside triphosphates can also be modified to cause alterations in the functional groups responsible for hydrogen bonding (*23*, *24*). Modifications to DNA and nucleotide pools could act in concert to synergistically decrease polymerization fidelity and cause a substantially higher frequency of mutagenesis. Although a wide variety of repair pathways function to avert such a catastrophe, their efficiency can be compromised if the cytotoxic insult overwhelms their collective activities. Indeed, this can be a significant complication in the treatment of various cancers as alkylating agents are widely used as chemotherapeutic modalities against these malignancies (*25*). In chemotherapy, these agents damage the DNA of cancer cells that are rapidly replicating and dividing. Unfortunately, this destruction also occurs in other rapidly replicating cells

† This research was supported through funding from the National Institutes of Health (CA118408) and the Skin Cancer Foundation to AJB.

* To whom correspondence should be addressed. Phone: (216) 368-4723. Fax: (216) 368-3395. E-mail: ajb15@cwru.edu.

‡ Department of Chemistry.

§ Department of Pharmacology.

10.1021/bi701328h CCC: $37.00
Published on Web 11/06/2007

such as bone marrow and gastrointestinal epithelia, which accounts for side effects including immunosuppression, nausea, and vomiting. A potentially more devastating complication is the risk of developing of a secondary cancer caused by the cytotoxic effects of these DNA-damaging agents (*26*).

In this paper we evaluate the hypothesis that inappropriate modifications to the templating nucleobase and incoming nucleotide can lead to a synergistic decrease in polymerase fidelity. This was achieved by quantifying the ability of the high-fidelity bacteriophage T4 DNA polymerase to incorporate and extend beyond an abasic site in the presence of various alkylated and modified purine analogues. These kinetic studies reveal that simple alkylation of dATP and dGTP significantly enhances promutagenic DNA synthesis by facilitating incorporation opposite an abasic site. The resulting structure−activity relationship provides a consistent theme in which the catalytic efficiency for incorporation opposite the non-instructional DNA lesion is influenced by the hydrophobic and aromatic properties of the incoming nucleotide. In addition, extension beyond the formed mispair is also facilitated by their enhanced base-stacking capabilities. Although many of these analogues are effectively incorporated opposite an abasic site, they do not show enhanced misincorporation opposite templating DNA. Collectively, these data indicate that the mechanism and biophysical forces used to misreplicate templating or non-instructional DNA lesions are inherently different.

MATERIALS AND METHODS

Materials. [γ-^{32}P]ATP was purchased from MP Biomedical (Irvine, CA). Unlabeled dNTPs (ultrapure) were obtained from Pharmacia. $MgCl_2$ and Trizma base were from Sigma. Urea, acrylamide, and bisacrylamide were from Aldrich. Oligonucleotides, including those containing a tetrahydrofuran moiety mimicking an abasic site, were synthesized by Operon Technologies (Alameda, CA). 2-APTP,[1] dITP, 8-oxo-dATP, 6-Cl-PTP, 6-Cl-2-APTP, 7-deaza-dATP, N^2-methyl-dGTP, O^6-methyl-dGTP, and N^6-methyl-dATP were obtained from TriLink BioTechnologies (San Diego, CA), while 7-deaza-dGTP was obtained from Sigma in greater than 99% purity. All other materials were obtained from commercial sources and were of the highest available quality. The exonuclease-deficient mutant of gp43 (Asp-219 to Ala mutation) was purified and quantified as previously described (*27*, *28*).

General Methods. Single-stranded and duplex DNA were purified and quantified as previously described (*29*). 5′-Ends of the primer and template strands were labeled using [γ-^{32}P]-ATP and T4 polynucleotide kinase (GibcoBRL). The assay buffer used in all kinetic studies consisted of 25 mM Tris−OAc (pH 7.5), 150 mM KOAc, and 10 mM 2-mercaptoethanol. All polymerization reactions were performed at 25 °C and were monitored by analysis of the products on 20% sequencing gels as described (*30*). Gel images were obtained with a Packard PhosphorImager using the Opti-Quant software supplied by the manufacturer. Product formation was quantified by measuring the ratio of ^{32}P-labeled extended and nonextended primer. The ratios of product formation are corrected for substrate in the absence of polymerase (zero point). Corrected ratios are then multiplied by the concentration of primer/template used in each assay to yield the total product. All concentrations are listed as final solution concentrations.

Determination of the Kinetic Rate and Dissociation Constants for dXTP Incorporation. The kinetic parameters, k_{pol} and K_d, for each dXTP were obtained by monitoring the rate of product formation using single-turnover reaction conditions. In these experiments, fixed amounts of gp43 exo$^-$ (1 μM) and DNA substrate (250 nM) were used while the concentration of dXTP was varied from 10 to 500 μM. Aliquots of the reaction were quenched into 200 mM EDTA, pH 7.4, at times ranging from 5 to 240 s. In some instances, time courses were generated using a rapid quench instrument as previously described (*22*). These experiments were likewise performed using single-turnover conditions in which 1 μM gp43 exo$^-$ and 250 nM DNA substrate were mixed against various concentrations of dNTP (10−500 μM) at time intervals ranging from 0.005 to 10 s. The reactions were quenched through the addition of 350 mM EDTA. Quenched samples were diluted 1:1 with sequencing gel load buffer, and the products were analyzed for product formation by denaturing gel electrophoresis. Data obtained for single-turnover rates in DNA polymerization were fit to eq 1, where

$$y = A(1 - e^{-k_{obsd}t}) + C \quad (1)$$

A is the burst amplitude, k_{obsd} is the first-order rate constant, t is time, and C is a defined constant. Data for the dependency of k_{obsd} versus dXTP concentration were fit to the equation describing a rectangular hyperbola (eq 2), where k_{obsd} is the

$$k_{obsd} = k_{pol}[dXTP]/K_d + [dXTP] \quad (2)$$

apparent first-order rate constant, k_{pol} is the maximal polymerization rate constant, K_d is the kinetic dissociation constant for dXTP, and [dXTP] is the concentration of nucleotide substrate.

Extension Beyond an Abasic Site. Single-turnover conditions were used to measure the rates of extension beyond a dXMP:abasic site mispair. gp43 exo$^-$ (1 μM) was incubated with 500 nM DNA (13/20SP-mer) in assay buffer containing EDTA (100 μM) and mixed with 100 μM dXTP and 10 mM magnesium acetate. After ~60 s, 900 μM dGTP (the correct dNTP for the next three positions) was added. Aliquots of the reactions were quenched with 500 mM EDTA at variable times (5−900 s) and analyzed as described above.

RESULTS AND DISCUSSION

Kinetic Parameters for Incorporation of Alkylated Purines Opposite an Abasic Site. The focus of this study is to

[1] Abbreviations: TBE, Tris−HCl/borate/EDTA; EDTA, ethylenediaminetetraacetate, sodium salt; dNTP, deoxynucleoside triphosphate; dXTP, unnatural deoxynucleoside triphosphate; 2-APTP, 2-amino-2′-deoxyadenosine 5′-triphosphate; dITP, 2′-deoxyinosine 5′-triphosphate; 6-Cl-PTP, 6-chloropurine-2′-deoxyadenosine 5′-triphosphate; 6-Cl-2-APTP, 6-chloro-2-amino-2′-deoxyriboside 5′-triphosphate; 7-deaza-dATP, 7-deaza-2′-deoxyadenosine 5′-triphosphate; 7-deaza-dGTP, 7-deaza-2′-deoxyguanosine 5′-triphosphate; N^2-methyl-dGTP, N^2-methyl-2′-deoxyguanosine 5′-triphosphate; O^6-methyl-dGTP, O^6-methyl-2′-deoxyguanosine 5′-triphosphate; N^6-methyl-dATP, N^6-methyl-2′-deoxyadenosine 5′-triphosphate; 5-NITP, 5-nitroindolyl-2′-deoxyriboside triphosphate; 5-PhITP, 5-phenylindolyl-2′-deoxyriboside triphosphate; gp43 exo$^-$, an exonuclease-deficient mutant of the bacteriophage T4 DNA polymerase.

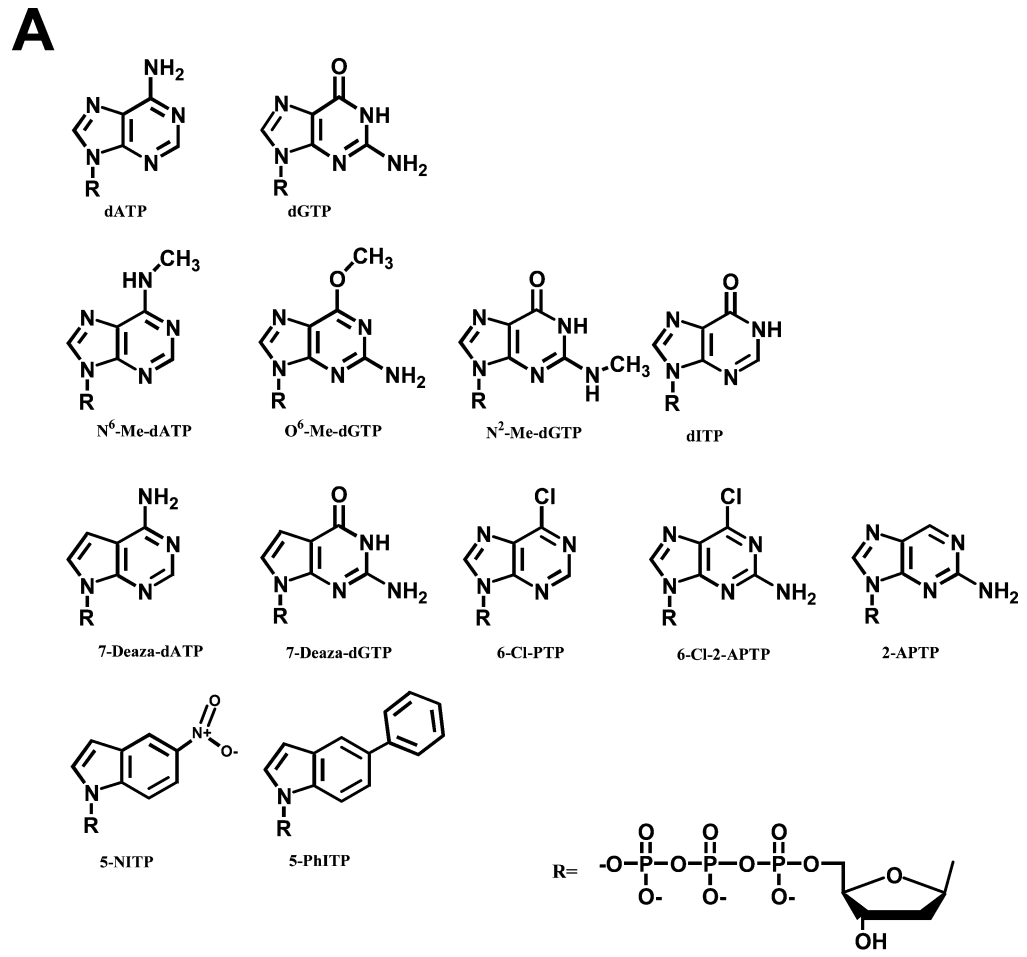

FIGURE 1: (A) Structures of 2′-deoxynucleoside triphosphates used or referred to in this study, i.e., dATP, dGTP, N^6-methyl-dATP, 6-Cl-PTP, dITP, O^6-methyl-dGTP, N^2-methyl-dGTP, 2-APTP, 6-Cl-2-APTP, 7-deaza-dATP, 7-deaza-dGTP, 5-NITP, and 5-PhITP. For convenience, R is used to represent the deoxyribose triphosphate portion of the nucleotides. (B) Defined DNA substrates used for kinetic analysis. "X" in the template strand denotes any of the four natural nucleobases or the presence of a tetrahydrofuran moiety that functionally mimics an abasic site.

understand the molecular mechanism for the misreplication of an abasic site (Figure 1A), a DNA lesion that can culminate from the alkylation of purines and pyrimidines (*3*−*5*). Upon encountering this non-instructional DNA lesion, most polymerases preferentially incorporate dATP and subsequently extend beyond the formed mispair (*16*−*20*) to propagate a potential genomic error. The question asked in this paper is whether promutagenic DNA synthesis can be exacerbated through modifications to both the DNA template *and* the incoming nucleoside triphosphate.

To evaluate this question, we examined whether subtle modifications to dATP or dGTP can influence the dynamics of misincorporation. The first analogue tested is N^6-methyl-dATP,[2] a modified purine that can arise through simple alkylation at the N6-position of adenine (Figure 1B). Representative data provided in Figure 2A illustrate the dependency on the rate constant in primer elongation as a function of N^6-methyl-dATP concentration. Each time course in primer elongation was fit to the equation defining a single-exponential process (eq 1) to obtain k_{obsd} values. The plot of k_{obsd} versus N^6-methyl-dATP concentration is hyperbolic (Figure 2B) and was fit to the equation describing a rectangular hyperbola to obtain a K_d of 190 ± 45 μM, a k_{pol} of 5.6 ± 0.6 s^{-1}, and a k_{pol}/K_d of 28 420 M^{-1} s^{-1}.

The 7-fold greater catalytic efficiency for N^6-methyl-dATP compared to dATP (28 420 M^{-1} s^{-1} versus 4300 M^{-1} s^{-1}, respectively) indicates that the modified nucleotide is more promutagenic than the parental nucleotide. The enhanced kinetic behavior for N^6-methyl-dATP does not arise from an increase in binding affinity as the K_d of 190 μM for N^6-methyl-dATP is ~5-fold higher than the K_d of 35 μM for dATP (*22*). Instead, the k_{pol} value of 5.6 s^{-1} for N^6-methyl-dATP is ~40-fold faster than that for dATP (0.15 s^{-1} (*22*)).

[2] Alkylating agents predominantly modify dATP at the heterocyclic nitrogens (N3 and N7) as well as at the exocyclic amino group (N6-position) (*6*). Although N3-alkylated dATP is well characterized, the formation and physiological consequences of N^6-methyl-dATP are poorly understood.

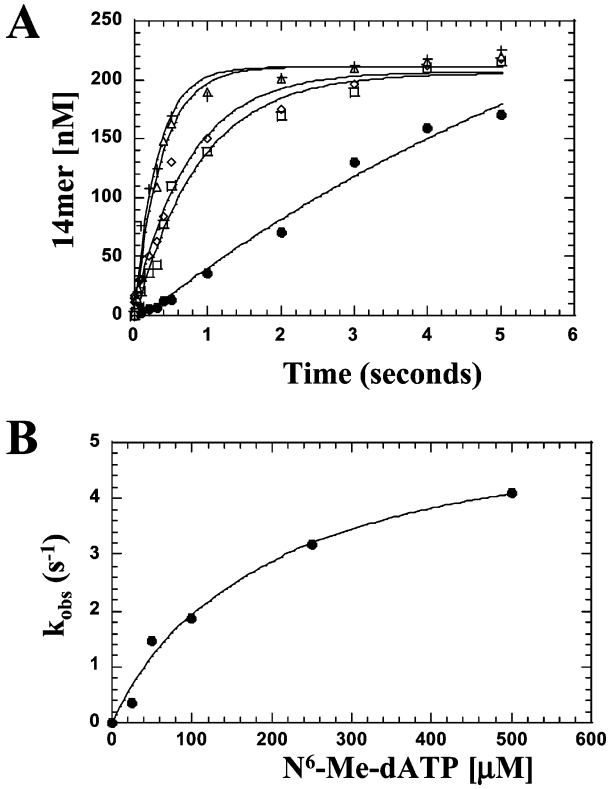

FIGURE 2: (A) Dependency of N^6-methyl-dATP concentration on the observed rate constant in primer elongation as measured using single-turnover conditions. The following concentrations of N^6-methyl-dATP were used: 25 μM (●), 50 μM (□), 100 μM (◇), 250 μM (+), and 500 μM (△). The solid lines represent the fit of each time course to a single-exponential process. (B) The observed rate constants for incorporation (●) were plotted against N^6-methyl-dATP concentration and fit to the equation defining a rectangular hyperbola to determine values corresponding to K_d, k_{pol}, and k_{pol}/K_d.

The dramatic enhancement in the k_{pol} value suggests that increasing the hydrophobicity and/or overall size of the nucleotide facilitates the conformational change step that precedes phosphoryl transfer.

We next evaluated whether alkylation of other natural nucleotides also increases their promutagenic potential. The incorporation of O^6-methyl-dGTP and N^2-methyl-dGTP opposite an abasic site was tested since alkylation at either position leads to an overall increase in size and hydrophobicity compared to those of dGTP (refer to Table 2). The catalytic efficiency for O^6-methyl-dGTP is ~30-fold greater compared to that of the incorporation of dGTP (compare 5400 M^{-1} s^{-1} with 180 M^{-1} s^{-1}, respectively).[3] Alkylation at the O6-position of dGTP leads to an effect similar to that observed with N^6-methyl-dATP, i.e., a significant increase in the k_{pol} value concomitant with decreased binding affinity. In fact, it is striking that the 40-fold faster k_{pol} value with O^6-methyl-dGTP versus dGTP (compare 0.98 s^{-1} with 0.023 s^{-1}, respectively) is identical to the 40-fold enhancement in k_{pol} values between N^6-methyl-dATP and dATP.

The ~3-fold higher catalytic efficiency for N^2-methyl-dGTP compared to dGTP also indicates that alkylation increases the potential for promutagenic synthesis opposite an abasic site. The enhanced catalytic efficiency is again caused by an increased k_{pol} value rather than an influence on binding affinity. At face value, the increased k_{pol} values coincide with changes associated with solvation energies between modified and unmodified nucleobases. However, this explanation is incomplete since the k_{pol} of 0.11 s^{-1} measured with N^2-methyl-dGTP is ~9-fold slower than that of 0.98 s^{-1} for O^6-methyl-dGTP. This difference corresponds to a relative change in Gibb's free energy ($\Delta\Delta G$) of 1.3 kcal/mol and is significantly less that the 2.3 kcal/mol difference in solvation energies between the two analogues (Table 1). Similar observations exist comparing alkylated nucleotides with their unmodified counterparts as the change in $\Delta\Delta G$ associated with solvation energies of the nucleotides does not equal the energetic differences associated with increases in the k_{pol} values. This analysis clearly indicates that other biophysical parameters must also contribute to account for the energetic differences. We propose that differences in the aromaticity of the nucleotides as manifest in the different tautomeric forms of N^2-methyl-dGTP versus O^6-methyl-dGTP influence their incorporation opposite the non-instructional lesion. This prediction is reasonable since changes in tautomeric form are known to influence the base-stacking capacity of a nucleotide (*31*, *32*).

This hypothesis was tested by measuring the kinetic parameters for dITP (Figure 1B), a nucleotide formed via the deamination of dATP. If hydrophobicity alone dictates incorporation efficiency opposite an abasic site, then the resulting ~5 kcal/mol decrease in the solvation energy associated with this modification should enhance the incorporation of dITP opposite the lesion. Contrary to this prediction, we find that dITP is incorporated very poorly opposite an abasic site with a k_{pol}/K_d value of 430 M^{-1} s^{-1}. In fact, the low k_{pol} of 0.044 s^{-1} and relatively high K_d of 103 μM are nearly identical to those for dGTP (k_{pol} = 0.023 s^{-1} and K_d = 130 μM (*22*)). Indeed, the striking similarity in the kinetic behavior of dITP and dGTP coincides with the similarities in tautomeric form.

The collective data set indicates that the aromatic nature of the nucleotide in addition to its hydrophobicity plays a significant role during translesion DNA synthesis to enhance the promutagenic replication of an abasic site. At the molecular level, this enhancement is achieved through increases in the k_{pol} value that reflects the enhanced base-stacking capabilities of the nucleotide. On the other hand, binding affinity appears to be adversely affected by any increase in the hydrophobic nature of the incoming nucleotide. As discussed below, one possibility is that the functional groups on dATP that provide hydrogen-bonding interactions are in fact essential for achieving optimal binding in the absence of templating information.

Kinetic Parameters for the Incorporation of Modified Purines Opposite an Abasic Site. We next tested the ability of gp43 exo$^-$ to incorporate various unnatural purine triphosphates such as 7-deaza-dATP, 6-Cl-PTP, and 6-Cl-2-APTP (Figure 1B) opposite an abasic site. The various atomic substitutions and permutations of functional groups allow us to further evaluate the role of hydrophobicity and aromatic interactions during translesion DNA synthesis. K_d and k_{pol} values for this series of purine analogue were measured as described above and are summarized in Table

[3] The magnitude of this effect for O^6-methyl-dGTP is greater than that for N^6-methyl-dATP. However, the larger magnitude for O^6-methyl-dGTP reflects the poor kinetics by which dGTP is incorporated opposite the abasic site.

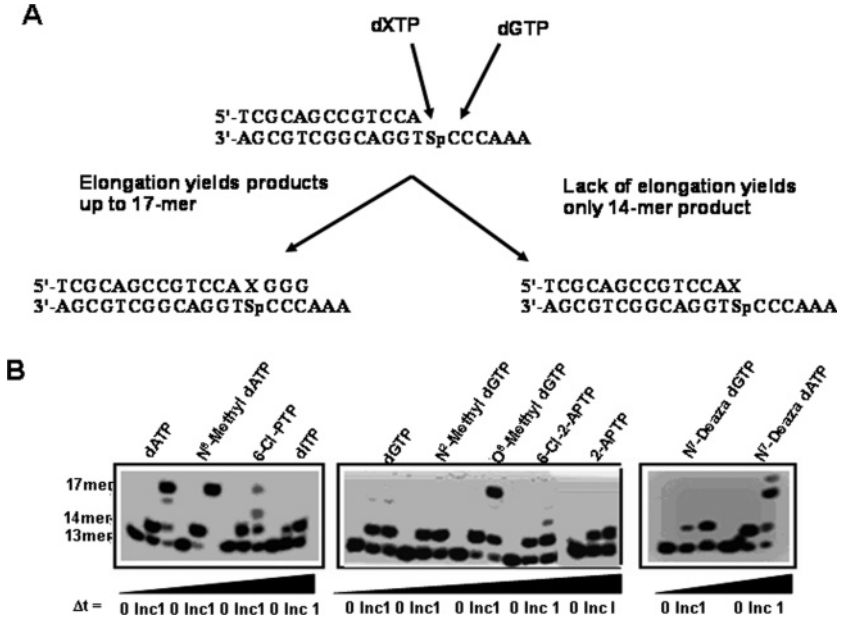

FIGURE 3: (A) Experimental paradigm used to measure insertion and extension beyond an abasic site lesion. A preincubated solution of 1 μM gp43 exo$^-$ and 500 nM 5′-labeled 13/20SP-mer was mixed with 50 μM dXTP to initiate the reaction. After 2 min, an aliquot of the reaction was quenched with 200 mM EDTA (denoted as "Inc") to measure insertion opposite the lesion. dGTP (900 μM) was then added, and aliquots of the reaction were quenched with 200 mM EDTA at 60 s. (B) Denaturing gel electrophoresis reveals that gp43 exo$^-$ extends beyond dATP, N^6-methyl-dATP, 6-Cl-PTP, O^6-methyl-dGTP, 6-Cl-2-APTP, and N^7-deaza-dATP when paired opposite an abasic site.

Table 1: Summary of Kinetic Parameters for the Incorporation of Modified Nucleotides Opposite an Abasic Site[a]

analogue	K_D (μM)	k_{pol} (s^{-1})	k_{pol}/K_D (M^{-1} s^{-1})	surface area[b] (Å^2)	dipole moment[b] (D)	solvation energy[b] (kcal/mol)	tautomeric form[c]
dATP[d]	35 ± 5	0.15 ± 0.01	4 300	143.0	2.38	−19.258	dATP
dGTP[d]	130 ± 5	0.023 ± 0.005	180	152.5	7.18	−26.009	dGTP
N^6-methyl-dATP	190 ± 45	5.6 ± 0.6	29 500	165.0	2.16	−16.322	dATP
O^6-methyl-dGTP	181 ± 35	0.98 ± 0.08	5 400	174.5	2.94	−19.998	dATP
N^2-methyl-dGTP	245 ± 68	0.12 ± 0.02	490	173.1	7.54	−22.306	dGTP
dITP	103 ± 14	0.044 ± 0.003	430	139.0	5.63	−21.790	dGTP
7-deaza-dATP	197 ± 40	1.4 ± 0.1	7 100	148.7	3.64	−17.846	dATP
7-deaza-dGTP	215 ± 91	0.11 ± 0.02	500	158.2	4.95	−24.247	dGTP
6-Cl-PTP	83 ± 16	0.28 ± 0.02	3 380	145.2	4.99	−16.449	dATP
6-Cl-2-APTP	71 ± 20	0.12 ± 0.01	1 700	158.7	4.83	−19.063	dATP
2-APTP	180 ± 23	0.23 ± 0.02	1 300	143.2	3.10	−19.142	dATP
5-NITP[e]	18 ± 3	126 ± 7	7 000 000	171.4	7.81	−7.381	NA[g]
5-PhITP[f]	14 ± 3	53 ± 4	3 800 000	223.2	3.31	−5.532	NA

[a] Assays were performed using 1 μM gp43 exo$^-$, 250 nM 13-20SP-mer, and variable concentrations of unnatural nucleotide in the presence of 10 mM Mg^{2+}. [b] Surface areas (used as an indicator of the relative size of the nucleobase), dipole moments (D), and solvation energies for each nucleobase were calculated using Spartan '04 software. [c] The tautomeric form refers to whether the purine analogue has the same tautomeric form as dATP or dGTP. [d] Values taken from ref *6*. [e] Values taken from ref *47*. [f] Values taken from ref *48*. [g] NA = not applicable

1. In general, modifications and/or atomic substitutions that increase the hydrophobicity of a nucleotide generally increase the rate constant for incorporation while reducing binding affinity opposite an abasic site. 7-Deaza-dATP provides a clear example of this kinetic phenomenon as the k_{pol} value of 1.5 s^{-1} is 10-fold faster than that of 0.15 s^{-1} for dATP (*22*) while the K_d value of 200 μM is ~6-fold higher than the K_d of 35 μM for dATP. Similar observations are obtained when the kinetic parameters for 7-deaza-dGTP are compared with those for dGTP.

The replacement of a hydrogen-bonding group with a non-hydrogen-bonding group does not substantially enhance the dynamics of translesion DNA synthesis. For example, 6-Cl-PTP shows only a modest 2-fold increase in k_{pol} despite a 2.81 kcal/mol reduction in solvation energy. The same modification of dGTP yields a larger effect as the k_{pol} of 0.12 s^{-1} measured for 6-Cl-2-APTP is 6-fold faster than that of 0.023 s^{-1} reported for dGTP (*22*). However, this increase is most likely caused by a combination of a change in hydrophobicity and a change in tautomeric form to resemble dATP, the preferred natural nucleotide.

Another unique feature is that the binding affinities for 6-Cl-PTP and 6-Cl-2-APTP are among the lowest measured for all the modified nucleotides tested in this study. As argued above, this result suggests that the 6-position of a purine may play an important role in the binding of natural and unnatural nucleotides during translesion DNA synthesis. This argument is supported by the high K_d value of 180 μM for 2-APTP, a constitutional analogue of dATP in which the N6 exocyclic amine is permutated to the 2-position (Figure 1B). Although this permutation has a strong effect on binding affinity, the influence on k_{pol} is minimal since the value of

Table 2: Summary of Kinetic Rate Constants for Extension beyond an Abasic Site Catalyzed by gp43 exo$^-$ [a]

dXTP	k_{ext} (s^{-1})	solvation energy (kcal/mol)	dXTP	k_{ext} (s^{-1})	solvation energy (kcal/mol)
		"dATP-like" Analogues			
dATP	0.25 ± 0.01	−19.258	6-Cl-2-APTP	0.033 ± 0.004	−19.063
7-deaza-dATP	0.32 ± 0.03	−17.846	6-Cl-PTP	0.031 ± 0.003	−16.449
N^6-methyl-dATP	0.71 ± 0.04	−16.322	2-APTP	ND[b]	−19.142
O^6-methyl-dGTP	0.092 ± 0.009	−22.306			
		"dGTP-like" Analogues			
dGTP	0.005 ± 0.001	−26.009	dITP	ND	−21.790
N^2-methyl-dGTP	ND	−19.998	7-deaza-dGTP	ND	−24.247

[a] Insertion and extension beyond an abasic site lesion were measured by preincubating gp43 exo$^-$ (1 μM) with 5′-labeled 13/20SP-mer (500 nM) and then mixing with a 50 μM concentration of modified nucleotide to initiate the reaction. After 2 min, an aliquot of the reaction was quenched with 200 mM EDTA (denoted as "Inc") to measure insertion opposite the lesion. dGTP (900 μM) was then added, and aliquots of the reaction were quenched with 200 mM EDTA at time intervals raging from 5 to 300 s. The generated time courses were fit to eq 1 to define k_{ext}, the rate constant for extension beyond the formed mispair. [b] ND = not detected.

Table 3: Summary of Kinetic Parameters for the Incorporation of Unnatural Nucleotides Opposite T and C[a]

	thymine			cytosine		
analogue	K_D (μM)	k_{pol} (s^{-1})	k_{pol}/K_D ($M^{-1}\,s^{-1}$)	K_D (μM)	k_{pol} (s^{-1})	k_{pol}/K_D ($M^{-1}\,s^{-1}$)
dATP[b]	10 ± 0.5	100 ± 10	10 000 000	ND	ND	<200[c]
dGTP	500 ± 200	0.04 ± 0.01	75	5 ± 2	47 ± 4	9 400 000
N^6-methyl-dATP	22 ± 13	82 ± 13	4 000 000	ND	ND	<40[c]
O^6-methyl-dGTP	465 ± 190	115 ± 27	247 310	116 ± 34	20.3 ± 2	175 000
N^2-methyl-dGTP	466 ± 177	0.07 ± 0.01	150	60 ± 35	1.7 ± 0.4	28 330
dITP	70 ± 19	0.080 ± 0.006	1 140	7 ± 5	49 ± 10	7 000 000
7-deaza-dATP	7 ± 2	80 ± 9	11 430 000	270 ± 90	9 ± 2	33 300
7-deaza-dGTP	850 ± 400	0.14 ± 0.04	164	2.4 ± 0.7	57 ± 4	23 750 000
2-APTP	25 ± 11	119 ± 20	4 760 000	90 ± 38	1.6 ± 0.2	18 100
6-Cl-PTP	25 ± 5	13 ± 1	520 000	395 ± 85	0.040 ± 0.003	105

[a] Assays were performed using 1 μM gp43 exo$^-$, 250 nM 13/20T-mer or 13/20C-mer, and variable concentrations of natural or modified nucleotide in the presence of 10 mM Mg^{2+}. [b] Values taken from ref *29*. [c] Estimates were calculated from the linear portion of the Michaelis−Menten plot.

0.23 s^{-1} is nearly identical, within error, to that of 0.15 s^{-1} for dATP. The similarity in tautomeric form and solvation energies between 2-APTP and dATP again correlates with the identical k_{pol} values.

Modified Purines Enhance Elongation beyond an Abasic Site. gp43 exo$^-$ extends beyond an abasic site only when either dAMP or dGMP is placed opposite the lesion (*22*, *33*). The dynamics of this process are proposed to reflect the positioning of either purine in an interhelical position that likely reflects their enhanced base-stacking capabilities compared to those of pyrimidines (*34*, *35*). This model leads to a testable prediction: *modified purines that possess enhanced base-stacking capabilities should be elongated more easily than their unmodified counterparts.* The biological ramifications of this model are obvious since the ability of a modified nucleotide to be elongated predicts a higher promutagenic potential. This model was tested using the experimental protocol outlined in Figure 3A that monitors the ability of gp43 exo$^-$ to extend beyond the various modified purines. Gel electrophoresis data provided in Figure 3B reveal that most hydrophobic nucleotides that resemble dATP are easily elongated. In contrast, analogues that are more hydrophilic and/or that resemble dGTP are more refractory to elongation. As summarized in Table 2, the rate constants for extension (k_{ext}) of analogues such as N^6-methyl-dATP and 7-deaza-dATP are ∼1.5−3-fold faster than that of dATP. This enhancement coincides with their predicted favorable base-stacking interactions opposite an abasic site.

Again, it is important to emphasize that the increase in base-stacking capacity depends upon the hydrophobic and aromatic nature of the nucleotide. This is apparent by examining the ability of gp43 exo$^-$ to elongate beyond N^2-methyl-dGTP. Although alkylation at the N2-position of dGTP increases its hydrophobicity, this does not lead to an enhancement in primer elongation. Furthermore, the lack of extension beyond dITP or N^7-deaza-dGTP is arguably caused by their weaker base-stacking capabilities that reflect reductions in their aromatic nature. Finally, the influence of aromaticity is also evident in the ∼20-fold increase in k_{ext} for O^6-methyl-dGTP that results in a change in tautomeric form caused by alkylation at the O6-position.

The lone exception to this proposed model is 2-APTP. Despite being similar to dATP with respect to tautomeric form and hydrophobicity, this analogue is not extended when paired opposite an abasic site. Although the molecular reason for this phenomenon is currently unknown, one possibility is that removal of a functional group at the C6-position prevents contacts between the minor groove of DNA and the DNA polymerase which are important for polymerase translocation (*36*, *37*). Consistent with this mechanism is the fact that 6-Cl-PTP is elongated ∼8-fold slower compared to dATP. These latter cases suggest that perturbations to the exocyclic amino group may influence the kinetics of elonga-

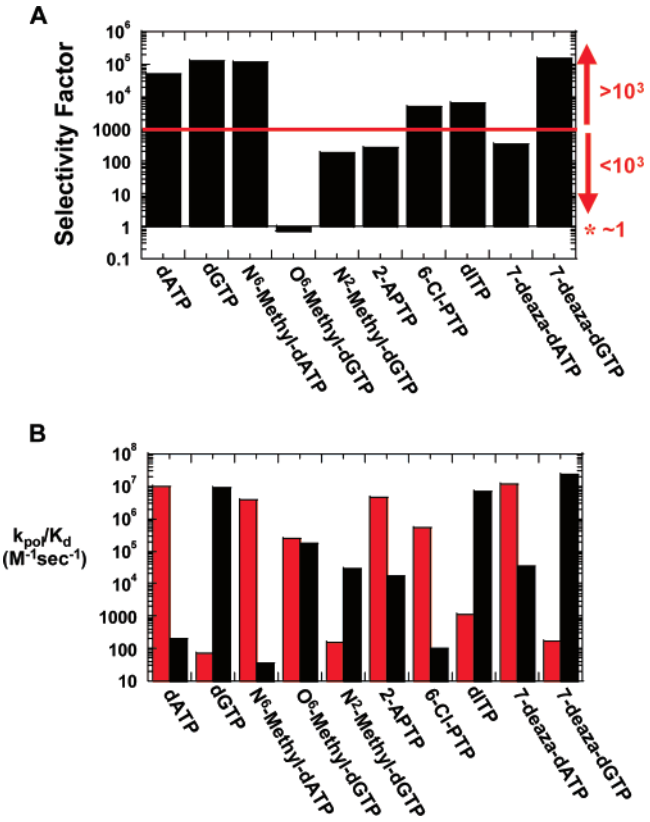

FIGURE 4: (A) Representation of the SF for each modified nucleotide for incorporation opposite thymine or cytidine. SF = $(k_{pol}/K_d)_{comp}/(k_{pol}/K_d)_{noncomp}$. Modified nucleotides are classified as those possessing high SF values of $>10^3$, those with low SF values of $<10^3$, and those with no selectivity (SF values of ~1). (B) k_{pol}/K_d values for each nucleotide as a function of templating nucleobase. Red bars represent incorporation opposite thymine, while black bars represent incorporation opposite cytosine.

tion. However, the collective data set demonstrates that the base-stacking properties of an incoming nucleotide increase its promutagenic potential by directly influencing incorporation and extension beyond an abasic site.

Influence of Hydrophobicity and Tautomeric Form on Misincorporation Opposite Templating Bases. We next questioned whether the enhanced base-stacking capacity of these modified nucleotides would also contribute toward facilitating misincorporation opposite templating nucleobases. This was initially tested by measuring K_d, k_{pol}, and k_{pol}/K_d values for this series of purine analogues opposite thymine or cytidine, which are predicted to be their complementary partners (summarized in Table 3). Figure 4A provides a graphical representation of the selectivity factor for each modified nucleotide for incorporation opposite thymine or cytidine. The selectivity factor (SF) is defined as the ratio of k_{pol}/K_d for nucleotide incorporation opposite its predicted complementary partner versus its noncomplementary partner (SF = $(k_{pol}/K_d)_{comp}/(k_{pol}/K_d)_{noncomp}$). This analysis allows us to classify the modified nucleotides into three distinct categories, those with high SF values of $>10^3$, those with low SF values of $<10^3$, and those with no selectivity (SF values of ~1). In addition, we provide a plot of the k_{pol}/K_d values for each nucleotide as a function of templating nucleobase (Figure 4B). This latter analysis is important since it indicates whether the SF values for various nucleotides are caused by an enhancement in the misreplication of a templating base or through diminution in incorporation opposite its predicted "correct" pairing partner or both. Distinguishing among these possibilities is important to accurately interpret how DNA synthesis is perturbed as a consequence of the nucleotide modifications.

Using this approach, we find that both unmodified nucleotides dATP and dGTP are very selective since their calculated SF values are $>10^4$. These high SF values are intuitively obvious since each nucleotide is predicted to exclusively interact with its complementary partner due to a combination of hydrogen-bonding interactions and steric constraints. Furthermore, these features are proposed to hinder their misincorporation opposite their noncognate partners. In this regard, it is surprising that certain analogues such as 7-deaza-dATP and N^2-methyl-dGTP, which have minimal perturbations toward steric fit and hydrogen-bonding interactions, have significantly lower SF values compared to their unmodified counterparts. This is interesting since both analogues are also incorporated opposite an abasic site with a relatively high efficiency. At face value, these coincidences suggest that simply increasing the hydrophobicity of a nucleotide will cause a unilateral decrease in fidelity. Indeed, this could describe the behavior of 7-deaza-dATP as the low SF value of 340 is caused by a significant increase in the misincorporation opposite cytidine while correct incorporation opposite thymine is left unperturbed. However, a universal "hydrophobic effect" is unlikely since the low SF value of 190 for N^2-methyl-dGTP is not caused by an increase for misinsertion opposite thymine. Instead, the reduced fidelity is caused by a surprisingly large decrease in incorporation opposite cytidine, its predicted complementary partner.

The best example arguing against a hydrophobic effect causing reduced fidelity in the presence of templating information is provided in the kinetic data for N^6-methyl-dATP. On one hand, this highly promutagenic nucleotide displays the highest catalytic efficiency for incorporation opposite an abasic site. However, it is remarkable that N^6-methyl-dATP maintains exquisite selectivity for incorporation opposite thymine versus cytidine. In fact, the SF value for N^6-methyl-dATP is actually 2-fold *higher* than that for dATP (compare 114 300 versus 50 000, respectively). This feature is not unique to N^6-methyl-dATP as similar trends are also observed with other hydrophobic analogues such as 7-deaza-dGTP and 6-Cl-dATP which maintain high SF values of $>10^3$.

One nucleotide that bears special emphasis is O^6-methyl-dGTP as this nucleotide owns the distinction of being the most promutagenic nucleotide identified in this study. With respect to translesion DNA synthesis, this nucleotide is effectively incorporated opposite an abasic site with a relatively high catalytic efficiency of 5400 M^{-1} s^{-1} (Table 1). In addition, O^6-methyl-dGTP is incorporated opposite thymine and cytidine with a low SF value of ~1, which indicates complete promiscuity for incorporation opposite pyrimidines. It is quite surprising that the similar catalytic efficiencies of 247 310 and 175 000 M^{-1} s^{-1} for incorporation opposite thymine and cytidine, respectively, occur through differential perturbations in the measured K_d and k_{pol} values. On one hand, the fast k_{pol} of 116 s^{-1} for incorporation opposite thymine likely reflects the fact that O^6-methyl-dGTP has the same tautomeric form as dATP.

This interpretation would support the fast k_{pol} value of ~1 s^{-1} measured for the incorporation of O^6-methyl-dGTP opposite an abasic site. However, the binding affinity of O^6-methyl-dGTP opposite thymine is dramatically reduced as manifest in the high K_d value of 465 μM. This suggests that ground-state binding opposite a templating base is influenced predominantly by hydrogen-bonding and/or steric-fit constraints rather than by base-stacking interactions.

We performed additional experiments measuring the incorporation of all modified purine triphosphates opposite noncognate partners, adenine and guanine (gel electrophoretic data and a summary of rate constants are provided as Supporting Information Figure 1). All of the modified purines are poorly incorporated opposite adenine or guanine as they possess estimated catalytic efficiencies of less than 10 M^{-1} s^{-1}. In fact, the rate constant for the incorporation of nearly all analogues is <0.01 s^{-1} even at nucleotide concentrations greater than 300 μM. In this regard, it is surprising that dATP is incorporated opposite adenine with a relatively high catalytic efficiency of 420 M^{-1} s^{-1} (Supporting Information Figure 2A). A similar phenomenon is observed for the incorporation of dGTP opposite guanine in which the overall catalytic efficiency is estimated to be ~100 M^{-1} s^{-1} (Supporting Information Figure 2B).

Collectively, the kinetic data obtained using these modified purine analogues do not provide evidence for a strong correlation between their hydrophobic and/or aromatic nature and the ability to form a mispair. In this regard, the dynamics by which a polymerase misreplicates a templating base appear to be vastly different from the dynamics for the misincorporation of a nucleotide opposite an abasic site. This conclusion has several important ramifications. First, differences in the underlying mechanism by which damaged DNA is misreplicated provide insight as to why the mutagenic spectra of closely related DNA-damaging agents are different. For example, dCTP and dTTP are typically incorporated opposite damaged nucleobases such as O^6-methylguanine and O^6-ethylguanine that contain small modifications (*38*, *39*). This implies that these lesions are replicated using features associated with classical hydrogen-bonding and steric-fit constraints much the same as for an unmodified guanine. However, the introduction of larger substituent groups at the O6-position of guanine gives rises to a different mutational spectrum in which dATP or dGTP is preferentially incorporated (*40*, *41*). In this latter case, the preferential incorporation of dATP argues that larger DNA lesions are replicated via a "transient abasic site intermediate". In any event, this information could be used to develop a predictive index for the mutagenic potential of other DNA-damaging agents. Another practical application is toward the rational design of antiviral agents that take advantage of low-fidelity replication catalyzed by most viral polymerases. Lower replication fidelity is generally tolerated by many viruses (*42*). However, the introduction of too many mutations, referred to as error catastrophe, may cause a loss of viral fitness and viability (*43*). This phenomenon has led to the development of a chemotherapeutic strategy termed "lethal mutagenesis" in which promutagenic nucleotides are used to increase the mutation frequency of viruses beyond viability to induce error catastrophe (*44*, *45*). While lethal mutagenesis represents an attractive antiviral strategy, it should be noted that controversy exists regarding the exact molecular mechanism by which certain nucleoside analogues such as ribavirin exert their antiviral effects.

CONCLUSIONS

In this paper we demonstrate that alkylated purine triphosphates can significantly enhance the promutagenic properties of an abasic site. The provided kinetic data yield further insights into the molecular mechanism of translesion synthesis. During replication of an abasic site, we argue that the enzymatic conformational change step (as reflected by the k_{pol} value) is influenced by the hydrophobic and aromatic nature of the incoming nucleotide.[4] This conclusion is consistent with our published model derived from characterizing the incorporation of various 5-substituted indolyl nucleoside triphosphates opposite this non-instructional DNA lesion (*46*). Non-natural nucleotides such as 5-NITP and 5-PhITP (Figure 1B) are incorporated opposite the abasic site with incredibly high catalytic efficiencies ($>10^6$ M^{-1} s^{-1}) (*47*, *48*). Both analogues have low affinity constants (K_d values <20 μM) coupled with fast incorporation rate constants (k_{pol} values >50 s^{-1}). The faster k_{pol} values measured with these 5-substituted indolyl nucleotides likely reflects their enhanced base-stacking capabilities that originate from their large π-electron surface area and hydrophobic nature.

The ability of various modified purines to be efficiently elongated has important biological ramifications, especially within the context of replicating non-instructional DNA lesions such as an abasic site. Simple alkylation of dATP or dGTP enhances the efficiency of translesion DNA synthesis that could cause a synergistic increase in mutagenesis under certain circumstances. The provocative implication of this conclusion is the potential risk of certain chemotherapeutic modalities to induce mutagenesis that may result in an additional prooncogenic event. Indeed, the administration of certain cytotoxic DNA-damaging agents such as temozolomide and cyclophosphamide is associated with a 10-fold higher risk of developing a secondary cancer (*49*).

Finally, the dynamics by which these modified purines are misincorporated are highly dependent upon the presence or absence of templating information. On one hand, increasing the hydrophobicity and aromaticity of a nucleotide leads to enhanced efficiency in incorporation and extension beyond an abasic site. However, a much more complex scenario exists during misinsertion opposite templating bases. In general, the catalytic efficiency for misinsertion depends more upon alterations in hydrogen-bonding interactions and shape complementarity as opposed to perturbations in hydrophobicity. Of course, unambiguous conclusions are difficult to make since modifying the functional group of an incoming nucleotide influences all three biophysical features to varying degrees. This last feature is important as it questions whether a truly universal mechanism of polymerization exists during the replication of normal versus damaged DNA. The data presented here suggest that different

[4] We have previously demonstrated that the incorporation of dATP and other unnatural nucleotides such as 5-NITP and 5-PhITP opposite an abasic site is limited by the conformational change step preceding phosphoryl transfer (*22*, *33*, *46*, *48*). However, we acknowledge this has not been conclusively demonstrated with the series of modified purines used in this study.

biophysical rules apply during template-dependent versus -independent DNA synthesis. Therefore, strict comparisons between the mechanisms of translesion DNA synthesis and correct DNA synthesis may be invalid. This dichotomy may explain the ease with which non-natural nucleotides can be designed to be efficiently incorporated opposite a non-instructional lesion while such efforts have proven more difficult in creating hybrid base pairs composed of natural and unnatural nucleotides.

SUPPORTING INFORMATION AVAILABLE

Gel electrophoretic data, a summary of kinetic rate constants, and catalytic efficiencies of dATP incorporated opposite adenine and dGTP incorporated opposite guanine. This material is available free of charge via the Internet at http://pubs.acs.org.

REFERENCES

1. Goodman, M. F., Creighton, S., Bloom, L. B., and Petruska, J. (1993) Biochemical basis of DNA replication fidelity, *Crit. Rev. Biochem. Mol. Biol. 28*, 83−126.
2. Quinto, I., Tenenbaum, L., and Radman, M. (1990) Genotoxic potency of monofunctional alkylating agents in *E. coli*: comparison with carcinogenic potency in rodents, *Mutat. Res. 228*, 177−185.
3. Encell, L., Shuker, D. E., Foiles, P. G., and Gold, B. (1996) The *in vitro* methylation of DNA by a minor groove binding methyl sulfonate ester, *Chem. Res. Toxicol. 9*, 563−567.
4. Abanobi, S. E., Columbano, A., Mulivor, R. A., Rajalakshmi, S., and Sarma, D. S. (1980) *In vivo* replication of hepatic deoxyribonucleic acid of rats treated with dimethyl-nitrosamine: presence of dimethylnitrosamine-induced O6-methylguanine, N7-methylguanine, and N3-methyladenine in the replicated hybrid deoxyribonucleic acid, *Biochemistry 19*, 1382−1387.
5. Marcelino, L. A., Andre, P. C., Khrapko, K., Coller, H. A., Griffith, J., and Thilly W. G. (1998) Chemically induced mutations in mitochondrial DNA of human cells: mutational spectrum of N-methyl-N′-nitro-N-nitrosoguanidine, *Cancer Res. 58*, 2857−2862.
6. Newbold, R. F., Warren, W., Medcalf, A. S. C., and Amos, J. (1980) Mutagenicity of carcinogenic methylating agents is associated with a specific DNA modification, *Nature 283*, 596−599.
7. Grevatt, P. C., Solomon, J. J., and Bhanot, O. S. (1992) *In vitro* mispairing specificity of O2-ethylthymidine, *Biochemistry 31*, 4181−4188.
8. Valko, M., Izakovic, M., Mazur, M., Rhodes, C. J., and Telser, J. (2004) Role of oxygen radicals in DNA damage and cancer incidence, *Mol. Cell. Biochem. 266*, 37−56.
9. Nakabeppu, Y., Sakumi, K., Sakamoto, K., Tsuchimoto, D., Tsuzuki, T., and Nakatsu, Y. (2006) Mutagenesis and carcinogenesis caused by the oxidation of nucleic acids, *Biol. Chem. 387*, 373−379.
10. Said, B., Ross, M. K., Salib, T., and Shank, R. C. (1995) Modulation of DNA adduct formation by successive exposures of DNA to small and bulky chemical carcinogens, *Carcinogenesis 16*, 3057−3062.
11. Schaaper, R. M., Glickman, B. W., and Loeb, L. A. (1982) Role of depurination in mutagenesis by chemical carcinogens, *Cancer Res. 42*, 3480−3485.
12. Dianov, G. L., Souza-Pinto, N., Nyaga, S. G., Thybo, T., Stevnsner, T., and Bohr, V. A. (2001) Base excision repair in nuclear and mitochondrial DNA, *Prog. Nucleic Acid Res. Mol. Biol. 68*, 285−297.
13. Krokan, H. E., Nilsen, H., Skorpen, F., Otterlei, M., and Slupphaug, G. (2000) Base excision repair of DNA in mammalian cells, *FEBS Lett. 476*, 73−77.
14. Boiteux, S., and Guillet, M. (2004) Abasic sites in DNA: Repair and biological consequences in *Saccharomyces cerevisiae*, *DNA Repair* (*Amsterdam*) *3*, 1−12.
15. Wilson, D. M., and Bohr, V. A. (2007) The mechanics of base excision repair, and its relationship to aging and disease, *DNA Repair* (*Amsterdam*) *6*, 544−559.
16. Schaaper, R. M., Kunkel, T. A., and Loeb, L. A. (1983) Infidelity of DNA synthesis associated with bypass of apurinic sites, *Proc. Natl. Acad. Sci. U.S.A. 80*, 487−491.
17. Boiteux, S., and Laval, J. (1982) Coding properties of poly(deoxycytidylic acid) templates containing uracil or apyrimidinic sites: *In vitro* modulation of mutagenesis by deoxyribonucleic acid repair enzymes, *Biochemistry 21*, 6746−6751.
18. Efrati, E., Tocco, G., Eritja, R., Wilson, S. H., and Goodman, M. F. (1997) Abasic translesion synthesis by DNA Polymerase beta violates the "A-rule". Novel types of nucleotide incorporation by human DNA polymerase beta at an abasic lesion in different sequence contexts, *J. Biol. Chem. 272*, 2559−2569.
19. Kroeger, K. M., Kim, J., Goodman, M. F., and Greenberg, M. M. (2006) Replication of an oxidized abasic site in Escherichia coli by a dNTP-stabilized misalignment mechanism that reads upstream and downstream nucleotides, *Biochemistry 45*, 5048−5056.
20. Fiala, K. A., Hypes, C. D., and Suo, Z. (2007) Mechanism of abasic lesion bypass catalyzed by a Y-family DNA polymerase, *J. Biol. Chem. 282*, 8188−8198.
21. Taylor, J. S. (2002) New structural and mechanistic insight into the A-rule and the instructional and non-instructional behavior of DNA photoproducts and other lesions, *Mutat. Res. 510*, 55−70.
22. Berdis, A. J. (2001) Dynamics of translesion DNA synthesis catalyzed by the bacteriophage T4 exonuclease-deficient DNA polymerase, *Biochemistry 40*, 7180−7191.
23. Kunz, B. A. (1988) Mutagenesis and deoxyribonucleotide pool imbalance, *Mutat. Res. 200*, 133−147.
24. Snow, E. T., and Mitra, S. (1988) Role of carcinogen-modified deoxynucleotide precursors in mutagenesis, *Mutat. Res. 200*, 157−164.
25. Murray, V. (1999) A survey of the sequence-specific interaction of damaging agents with DNA: emphasis on antitumor agents, *Prog. Nucleic Acid Res. Mol. Biol. 63*, 367−415.
26. Allan, J. M., and Travis, L. B. (2005) Mechanisms of therapy-related carcinogenesis, *Nat. Rev. Cancer 5*, 943−955.
27. Frey, M. W., Nossal, N. G., Capson, T. L., and Benkovic, S. J. (1989) Construction and Characterization of a bacteriophage T4 DNA polymerase deficient in 3′ → 5′ exonuclease activity, *Proc. Natl. Acad. Sci. U.S.A. 90*, 2579−2583.
28. Rush, J., and Konigsberg, W. H. (1989) Rapid purification of over expressed T4 DNA polymerase, *Prep. Biochem. 19*, 329−340.
29. Capson, T. L., Peliska, J. A., Kaboord, B. F., Frey, M. W., Lively, C., Dahlberg, M., and Benkovic, S. J. (1992) Kinetic characterization of the polymerase and exonuclease activities of the gene43 protein of bacteriophage T4, *Biochemistry 31*, 10984−10994.
30. Mizrahi, V., Benkovic, P. A., and Benkovic, S. J. (1986) Mechanism of DNA polymerase I: Exonuclease/polymerase activity switch and DNA sequence dependence of pyrophosphorolysis and misincorporation reactions, *Proc. Natl. Acad. Sci. U.S.A. 83*, 5769−5773.
31. Mignon, P., Loverix, S., Steyaert, J., and Geerlings, P. (2005) Influence of the $\pi-\pi$ interaction on the hydrogen bonding capacity of stacked DNA/RNA bases, *Nucleic Acids Res. 33*, 1779−1789.
32. Harris, V. H., Smith, C. L., Cummins, W., Hamilton, A. L., Adams, H., Dickman, M., Hornby, D. P., and Williams, D. M. (2003) The effect of tautomeric constant on the specificity of nucleotide incorporation during DNA replication: support for the rare tautomer hypothesis of substitution mutagenesis, *J. Mol. Biol. 326*, 1389−1401.
33. Hays, H., and Berdis, A. J. (2002) Manganese substantially alters the dynamics of translesion DNA synthesis, *Biochemistry 41*, 4771−4778.
34. Kalnik, M. W., Chang, C.N., Johnson, F., Grollman, A. P., and Patel, D. J. (1989) NMR studies of abasic sites in DNA duplexes: deoxyadenosine stacks into the helix opposite acyclic lesions, *Biochemistry 28*, 3373−3383.
35. Cuniasse, P., Fazakerley, G. V., Guschlbauer, W., Kaplan, B. E., and Sowers, L. C. (1990) The abasic site as a challenge to DNA polymerase. A nuclear magnetic resonance study of G, C and T opposite a model abasic site, *J. Mol. Biol. 213*, 303−314.
36. Morales, J. C., and Kool, E. T. (2000) Functional hydrogen-bonding map of the minor groove binding tracks of six DNA polymerases, *Biochemistry 39*, 12979−12988.
37. Matsuda, S., Henry, A. A., Schultz, P. G., and Romesberg, F. E. (2003) The effect of minor-groove hydrogen-bond acceptors and donors on the stability and replication of four unnatural base pairs, *J. Am. Chem. Soc. 125*, 6134−6139.

38. Spratt, T. E., and Levy, D. E. (1997) Structure of the hydrogen bonding complex of O6-methylguanine with cytosine and thymine during DNA replication, *Nucleic Acids Res. 25*, 3354−3361.
39. Perrino, F. W., Blans, P., Harvey, S., Gelhaus, S. L., McGrath, C., Akman, S. A., Jenkins, G. S., LaCourse, W. R., and Fishbein, J. C. (2003) The N2-ethylguanine and the O6-ethyl- and O6-methylguanine lesions in DNA: contrasting responses from the "bypass" DNA polymerase eta and the replicative DNA polymerase alpha, *Chem. Res. Toxicol. 16*, 1616−1623.
40. Perlow, R. A., and Broyde, S. (2002) Toward understanding the mutagenicity of an environmental carcinogen: Structural insights into nucleotide incorporation preferences, *J. Mol. Biol. 322* (2), 291−309.
41. Nivard, J. M. M., Pastink, A., and Vogel, W. E. (1992) Molecular analysis of mutations induced in the *vermilion* gene of Drosophila melanogaster by methyl methanesulfonate, *Genetics 131*, 673−682.
42. Svarovskaia, E. S., Cheslock, S. R., Zhang, W. H., Hu, W. S., and Pathak, V. K. (2003) Retroviral mutation rates and reverse transcriptase fidelity, *Front. Biosci. 8*, d117−134.
43. Anderson, J. P., Daifuku, R., and Loeb, L. A. (2004) Viral error catastrophe by mutagenic nucleosides, *Annu. Rev. Microbiol. 58*, 183−205.
44. Loeb, L. A., Essigmann, J. M., Kazazi, F., Zhang, J., Rose, K. D., and Mullins, J. I. (1999) Lethal mutagenesis of HIV with mutagenic nucleoside analogs, *Proc. Natl. Acad. Sci. U.S.A. 96*, 1492−1497.
45. Crotty, S., Maag, D., Arnold, J. J., Zhong, W., Lau, J. Y., Hong, Z., Andino, R., and Cameron, C. E. (2000) The broad-spectrum antiviral ribonucleoside ribavirin is an RNA virus mutagen, *Nat. Med. 6*, 1375−1379.
46. Devadoss, B., Lee, I., and Berdis, A. J. (2007) Is a thymine dimer replicated via a transient abasic site intermediate? A comparative study using non-natural nucleotides, *Biochemistry 46*, 4486−4498.
47. Reineks, E. Z., and Berdis, A. J. (2004) Evaluating the contribution of base stacking during translesion DNA replication, *Biochemistry 43*, 393−404.
48. Zhang, X., Lee, I., and Berdis, A. J. (2005) The use of nonnatural nucleotides to probe the contributions of shape complementarity and pi-electron surface area during DNA polymerization, *Biochemistry 44*, 13101−13110.
49. Smith, M. A., McCaffrey, R. P., and Karp, J. E. (1996) The secondary leukemias: challenges and research directions, *J. Natl. Cancer Inst. 88*, 407−418.

BI701328H